UDC [541.123.6+536]:546.22/23

PHASE EQUILIBRA IN THE $Ag_2Se–Ag_8GeSe_6–Ag_8SiSe_6$ SYSTEM AND CHARACTERIZATION Of the $Ag_8Si_{1-x}Ge_xSe_6$ SOLID SOLUTIONS

[1]G.M. Ashirov, [1]K.N. Babanly, [1]L.F. Mashadiyeva, [2]Y.A. Yusibov, [1]M.B. Babanly

[1]Acad. M. Nagiyev Institute of Catalysis and Inorganic Chemistry,
113, H.Javid ave, AZ 1143, Baku, Azerbaijan
[2]Ganja State University,
429, Heydar Aliyev ave., Ganja, Azerbaijan
e-mail: leylafm76@gmail.com

Received 07.06.2023
Accepted 10.08.2023

Abstract: *Phase equilibria in the $Ag_2Se–Ag_8SiSe_6–Ag_8GeSe_6$ system were studied by differential thermal analysis and X-ray diffraction thechnique. Based on the experimental results and literature data, the projection of the liquidus surface of the $Ag_2Se–Ag_8SiSe_6–Ag_8GeSe_6$ system, the isothermal section at 300 K and some polythermal sections of the phase diagram were constructed. It was determined that continuous series of solid solution are formed based on high-temperature cubic modification and limited solid solution areas are formed based on low-temperature modification of initial compounds on the $Ag_8SiSe_6–Ag_8GeSe_6$ side of concentration triangle. The formation of solid solutions leads to a sharp decreasing of polymorphic transition temperatures of ternary compounds and stabilization of high-temperature phases at room temperature. The liquidus surface of the $Ag_2Se–Ag_8SiSe_6–Ag_8GeSe_6$ system consists of 2 areas reflecting the initial crystallization of α'-phase based on HT-Ag_2Se and HT-$Ag_8Si_{1-x}Ge_xSe_6$ solid solutions. The obtained new phases are of interest as environmentally safe materials with thermoelectric properties and mixed ion-electron conductivity.*

Keywords: *Argyrodite family compounds, silver-germanium selenide, silver-silicon selenide, phase equilibria, liquid surface, solid solutions, T-x diagram, crystal lattice parameters.*
DOI: 10.32737/2221-8688-2023-3-229-241

1. Introduction

Complex copper and silver chalcogenides with germanium subgroup elements are valuable functional materials [1-3]. Among these compounds, synthetic analogues of the mineral argyrodite with the formula A_8BX_6 (A-Cu, Ag; B^{IV}-Si, Ge, Sn; X-S, Se, Te) are widely studied as environmentally safe materials with high thermoelectric figure of merit at medium temperatures [4-12]. Some of these compounds exhibit both photovoltaic and optical properties [13-17]. Most of the argyrodite family compounds have ionic conductivity due to the high mobility of Cu^+ (Ag^+) cations, which makes them very promising for use in preparing of photoelectrode materials, electrochemical solar energy converters, and ion-selective sensors [18-22].

It is known that the search and study of new multicomponent materials is based on information about the phase equilibrium of the corresponding systems and the thermodynamic properties of the phases formed in them [23-29]. Most compounds of the argyrodite family have polymorphic transitions at low temperatures. As a rule, their high-temperature modifications are crystallized in a cubic structure, while their low-temperature phases have lower symmetry. Low-temperature modifications of some representatives of this class are also isostructural. This increases the possibility of the formation of solid solutions of different structures in the systems based on argyrodite analogues. In a series of works [30-37], phase equilibria in systems consisting of argyrodite

phases were studied and new phases with variable composition were discovered in them.

The present study aimed to obtain a picture of phase equilibria in the the Ag_2Se–Ag_8GeSe_6–Ag_8SiSe_6 composition of the Ag_2Se–$GeSe_2$–$SiSe_2$ quasiternary system.

The started compounds of the studied Ag_2Se–Ag_8GeSe_6–Ag_8SiSe_6 system have been sufficiently studied. The Ag_2Se compound melts congruently at 1173K and undergoes a polymorphic transition at 406K [38]. Ag_8SiSe_6 compound also melts congruently. Different authors give sharply different values of its melting point. Authors of [39, 40] define melting temperature at 1203 K. In [41] and [42] showed temperture 1258 K and 1268 K, respectively. The polymorphic transition temperatures of this compound are 315, 354 K, respectively [43]. The low-temperature modification is tetragonal (Sp.gr. *I-4m2*, *a* = 0.7706, *b* =1.10141 nm) [39, 40], the intermediate modification (IT) is simple cubic (Sp.gr. $P4_232$, *a* = 1.087 nm) [20] and high-temperature modification has a face-centered cubic structure (Sp.gr. *F-43m*, *a* = 1.09413 nm) [39, 40]. The compound Ag_8GeSe_6 melts congruently at 1176 K and has a polymorphic transformation at 321 K [40]. The low-temperature modification has an orthorhombic (Sp.gr. $Pmn2_1$, a = 0.78235, b = 0.77126, c = 1.08854 nm) [44] and the high-temperature modification has a cubic (Sp.gr. *F-43m*, *a* = 1.09931 nm) structure [9].

Ag_2Se-Ag_8GeSe_6 and Ag_2Se-Ag_8SiSe_6 sides of the Ag_2Se–Ag_8GeSe_6–Ag_8SiSe_6 solids triangle are quasi-binary and form a eutectic diagram. In the Ag_2Se-Ag_8GeSe_6 system, the eutectic crystallizes at 1103 K [40, 45, 46], and in the Ag_2Se-Ag_8SiSe_6 system at 1113 K [39], 1123 K [40], 1073 K [41]. Another boundary system Ag_8GeSe_6-Ag_8SiSe_6 has not been studied.

2. Experiment part

2.1. Synthesis

Ag_2Se, Ag_8SiSe_6 and Ag_8GeSe_6 compounds were first synthesized for conducting research. The synthesis was carried out by melting stoichiometric mixtures of the corresponding simple substances with high purity in quartz ampoules under vacuum conditions (10^{-2}Pa). Since the saturated vapor pressure of selenium ($T_{boil.}$=958 K) at the melting temperature of all three compounds is high, their synthesis was carried out in a two-zone mode in an inclined furnace. The temperature of the furnace was gradually raised and heated to a temperature of 40-50 K above the melting point of the synthesized compound. A part of the ampoule outside the oven is constantly cooled. Due to the process of cooling with water for 2-3 hours, the selenium accumulated in the form of steam at the end of the ampoule was condensed and sent to the reaction zone, and after the absorption of most selenium, the ampoule was completely inserted into the furnace. After keeping in the oven for 4-5 hours, it was gradually cooled by disconnecting the oven from the power source.

The synthesized compounds were identified by differential thermal analysis (DTA) and X-ray diffraction analysis (XRD). Experimental DTA results for Ag_2Se and Ag_8GeSe_6 compounds showed that their temperatures of polymorph transition and melting corresponde to the above literature data [38, 40]. Three endothermic effects were detected on the heating DTA curve of Ag_8SiSe_6 compound. Small peaks corresponding to 315 K and 355 K represent polymorphic transformations, and an intense peak at 1278 K reflects the melting point. These results agree with the data in [43]. X-ray phase analysis confirms the homogeneity of the synthesized samples and coincides with the diffraction patterns given in the literature for RT-modification of compounds [9, 20, 39, 30, 44].

Alloys of the Ag_2Se–Ag_8GeSe_6–Ag_8SiSe_6 system were prepared by melting the mixtures of the primary compounds in different proportions in vacuumed quartz ampoules. To bring the samples to equilibrium, they were thermally treated for a long time (500 h) at 900 K. Two samples were prepared for each composition in the Ag_8GeSe_6–Ag_8SiSe_6 system, one of which was gradually cooled in a furnace disconnected from the current source after thermal treatment, and the other was annealed by dropping the ampoule in cold water below 900 K.

2.2. Analysis

All the alloys were analyzed using powder XRD and DTA techniques. Powder XRD analysis was performed in a Bruker D2 PHASER diffractometer using CuKα_1 radiation within the scanning range of 2θ=5÷75. DTA measurements were recorded with a "Netzsch 404 F1 Pegasus system" differential scanning calorimeter (under flowing argon atmosphere) and a multichannel device based on the electronic "TC-08 thermocouple data logger" (in sealed quartz tubes). The measurement results were processed using the NETZSCH Proteus Software. The temperature measurement accuracy was within ±2 K.

3. Results and discussion

Based on the obtained experimental results and literature data on the Ag_2Se–Ag_8GeSe_6 and Ag_2Se–Ag_8SiSe_6 systems [39-41, 45, 46], we obtained a detailed description of the phase equilibrium in the Ag_2Se–Ag_8GeSe_6–Ag_8SiSe_6 system.

3.1. Border section of Ag_8SiSe_6 – Ag_8GeSe_6

Based on DTA and XRD results, the phase diagram of Ag_8SiSe_6-Ag_8GeSe_6 system was constructed (Figure 1). As can be seen, in this system there is a continuous solid solution (δ-phase) between the high-temperature modifications of the initial compounds.

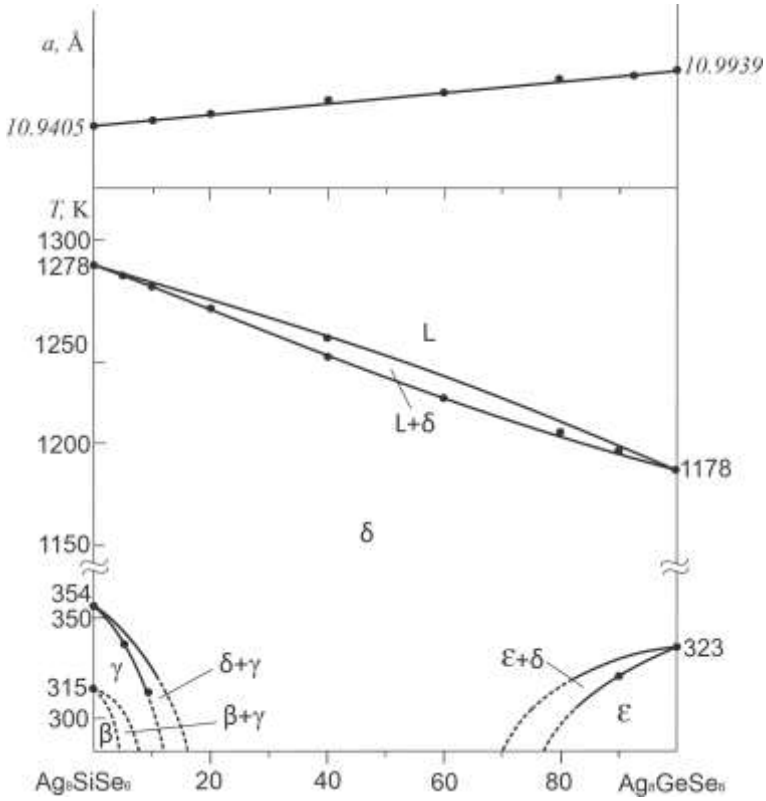

Fig. 1. Phase diagram of Ag_8SiSe_6-Ag_8GeSe_6 system and composition dependence of crystal lattice parameters of HT-$Ag_8Si_{1-x}Ge_xSe_6$ solid solutions.

Based on the low-temperature (β) and medium-temperature (γ) modifications of the Ag_8SiSe_6 compound, as well as the low-temperature modification (ε) of the Ag_8GeSe_6 compound, limited solid solution areas are formed. It can be seen from the phase diagram that the formation of solid solutions is accompanied by a decrease in the polymorphic transformation temperatures of the primary compounds. This leads to the widening of the temperature range in which the high-temperature ion-conducting δ-phase exists and

its stability at room temperature and below in the range of 15-70 mol% Ag_8GeSe_6.

Table 1. Crystal lattice parameters of HT-$Ag_8Si_{1-x}Ge_xSe_6$ solid solutions

Composition, mol% Ag_8GeSe_6	**Lattice parameters, 900 K ; (Cubic, F-43m) *a*, Å**
Ag_8SiSe_6	10.9405
10	10.9485
20	10.9528
40	10.9665
60	10.9772
80	10.9812
90	10.9884
Ag_8GeSe_6	10.9939

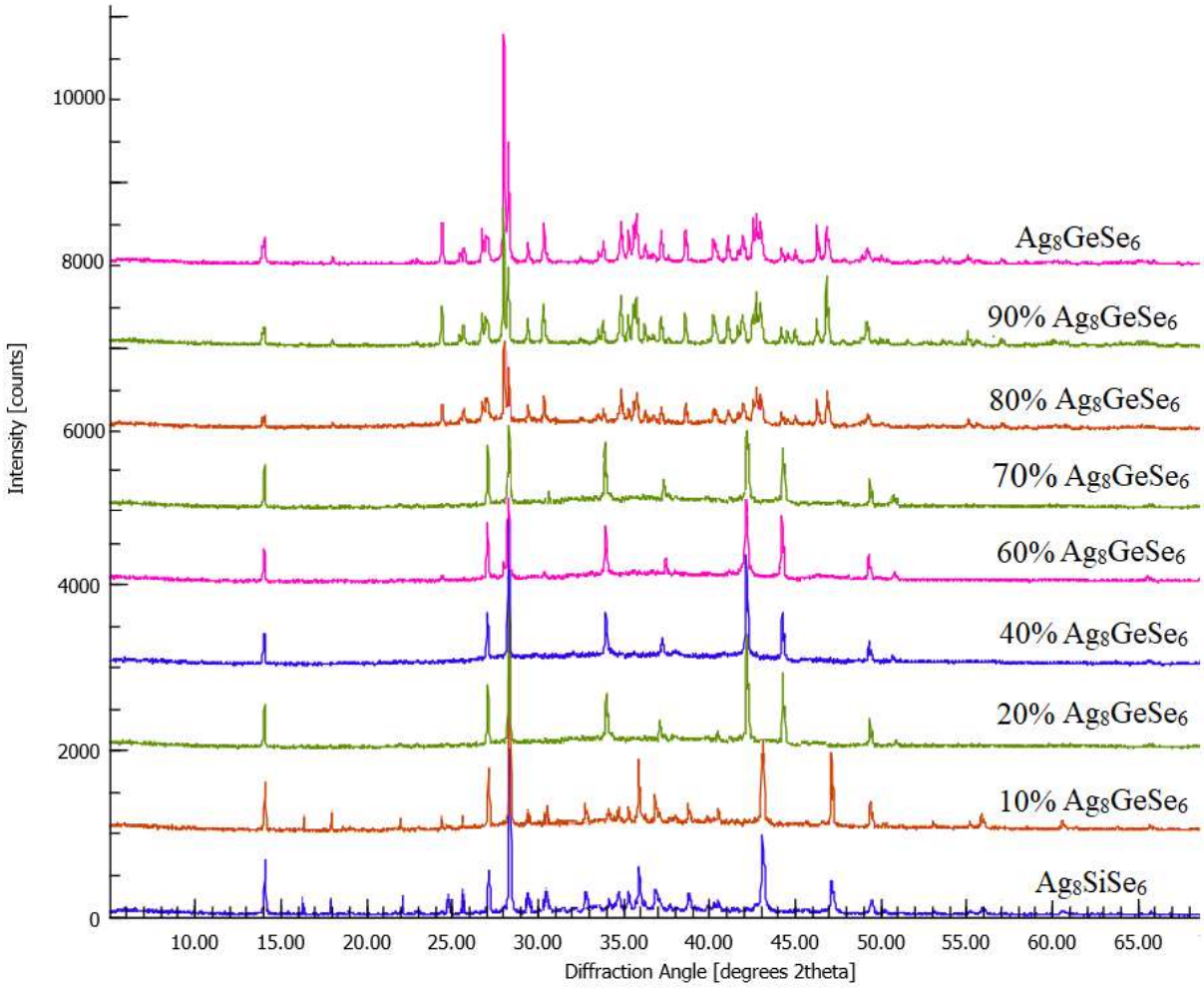

Fig. 2. X-ray diffraction patterns of Ag_8SiSe_6-Ag_8GeSe_6 system alloys (room temperature).

Fig. 2 shows the powder diffraction patterns of slowly cooled samples after thermal treatment. As can be seen, the diffraction patterns of the samples containing 90 and 80 mol% Ag_8GeSe_6 are qualitatively the same as pure RT-Ag_8GeSe_6, while the diffractograms of the samples belonging to the 20-70 mol% Ag_8GeSe_6 interval are similar to the cubic HT-modifications of the original compounds. Finally, the sample with 10 mol% Ag_8GeSe_6 has the same diffraction pattern as IT-Ag_8SiSe_6. These results confirm the phase diagram.

XRD results of samples quenched from 900 K are shown in Figure 3. It is clear that the diffractograms of the initial compounds and all intermediate samples are qualitatively the same and have a characteristic diffraction pattern for cubic structure. This confirms the formation of continuous δ-solid solutions in the system.

Lattice parameters of high-temperature modifications of ternary compounds and high-temperature solid solutions formed between them were calculated using the TOPAS 3.0 computer program, and the results are listed in Table 1.

Fig. 1 also shows the composition dependence graph of lattice parameters of HT-$Ag_8Si_{1-x}Ge_xSe_6$ solid solutions. As can be seen, the lattice parameters of solid solutions increase linearly with Ge substitution and follow Vegard's rule.

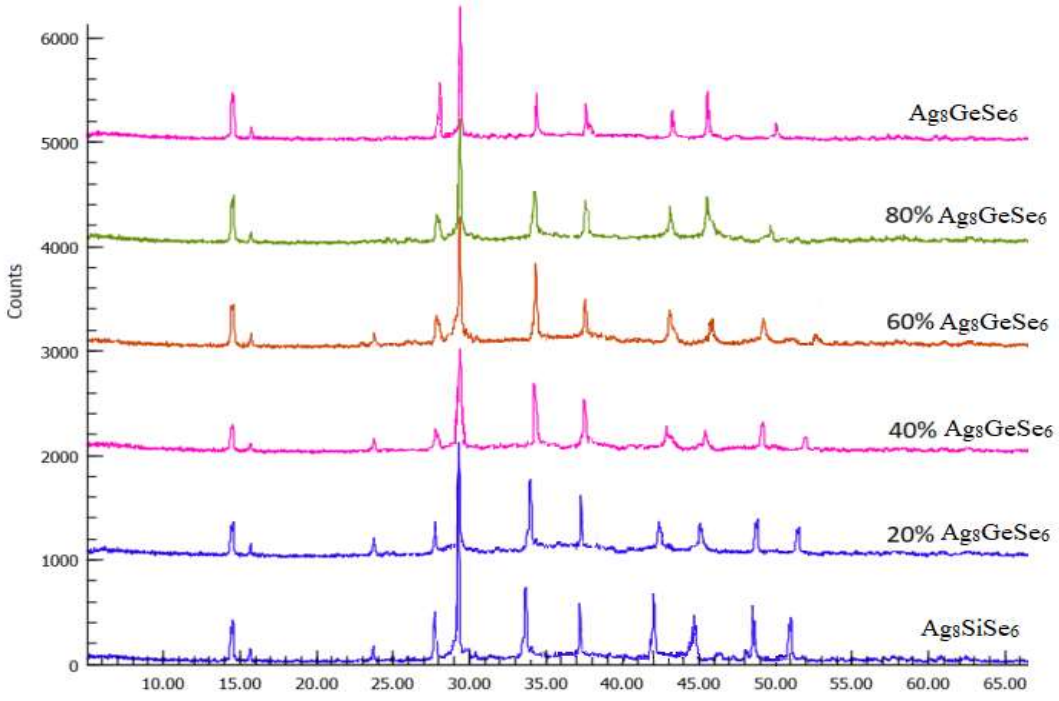

Fig. 3. X-ray diffraction patterns of Ag_8SiSe_6-Ag_8GeSe_6 samples quenched at 900K.

3.2 Solid phase equilibria of the $Ag_2Se–Ag_8GeSe_6–Ag_8SiSe_6$ system.

In Figure 4, the solid solutions formed in the $Ag_8GeSe_6–Ag_8SiSe_6$ system form connode lines with RT-Ag_2Se(α-phase) and with each other. Boundary connode lines divide the system into 10 heterogeneous areas. Sevenareas are two-phase (α+β, α+γ, α+δ, α+ε, β+γ, γ+δ, δ+ε), and three fields are three-phase (α+β+γ, α+γ +δ, α+ε+δ). The noted phase fields were confirmed by the XRD. Figure 5 shows the powder diffractograms of several mixtures.

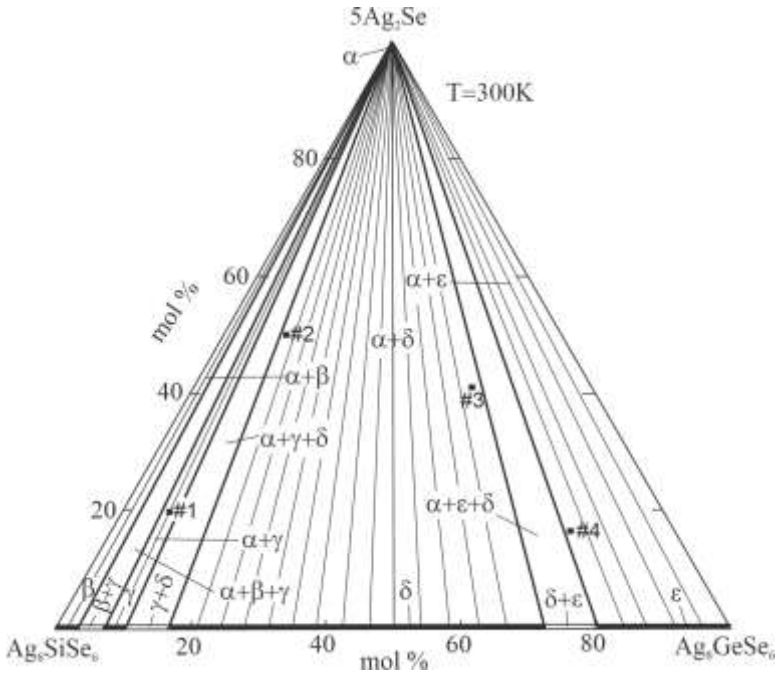

Fig. 4. İsothermal section at 300K

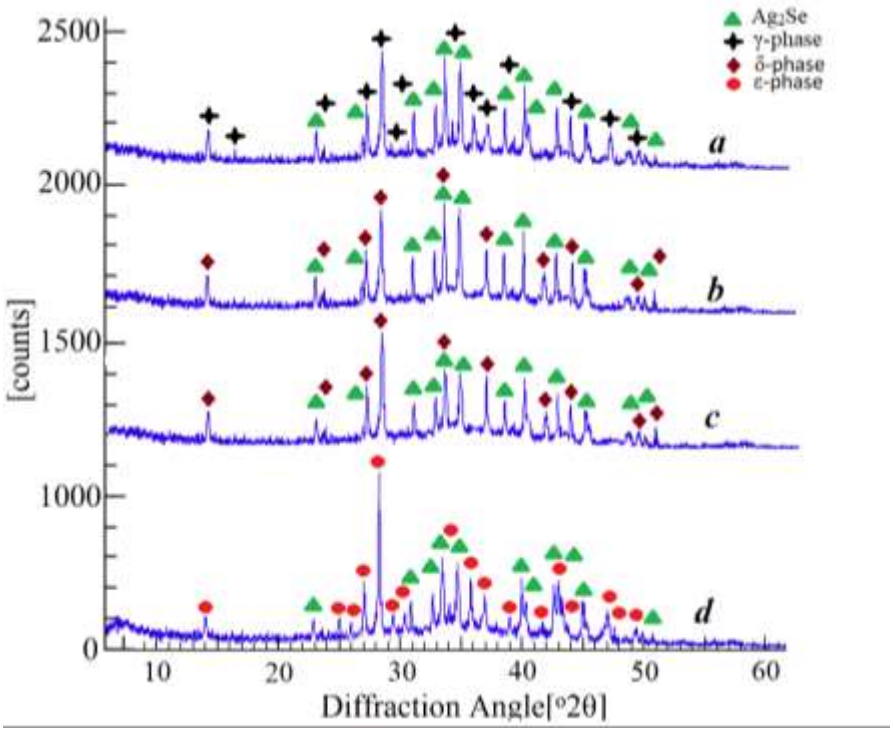

Fig. 5. Powder XRD patterns (300 K) of Ag_2Se-Ag_8SiSe_6 – Ag_8GeSe_6 alloys: (a) alloy - #1, (b) alloy #2, (c) alloy #3 and (d) alloy #4 in Fig.4

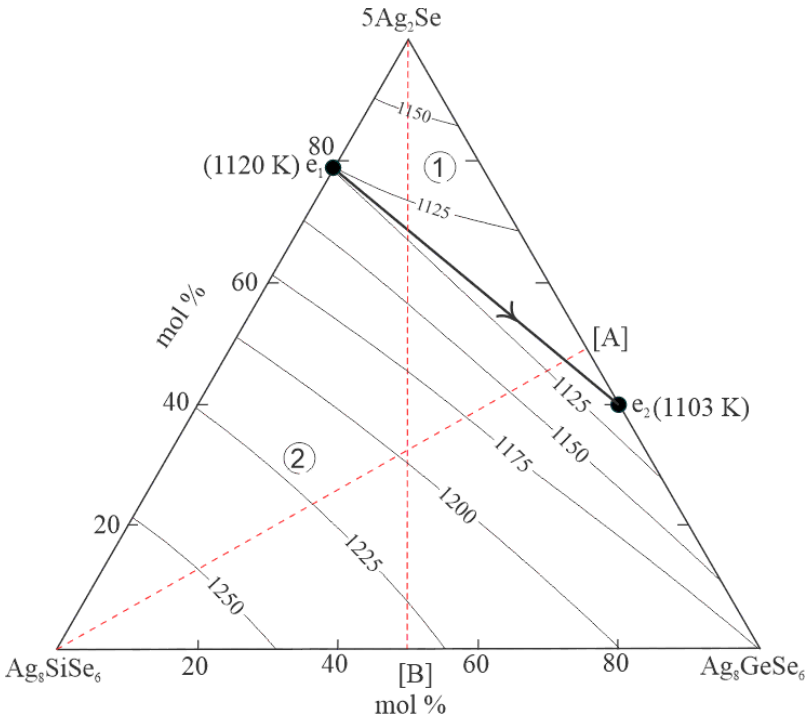

Fig. 6. Projection of the liquidus surface and studied polythermal sections of the Ag_2Se–Ag_8GeSe_6–Ag_8SiSe_6 system. Primary crystallization area: 1 (α'), 2 (δ). **Broken lines indicate studied vertical sections.*

3.3. Projection of the liquidus surface of the Ag_2Se–Ag_8GeSe_6–Ag_8SiSe_6 system

The projection of the liquidus surface of this system consists of two areas (Fig. 6). One of them corresponds to the initial crystallization of the α' solid solution based on the high-temperature modification of the Ag_2Se compound, and the second to the δ phase. These areas are bounded by the e_1e_2 curve reflecting the monovariant eutectic equilibrium (eutectic coordinates are 60 mol% Ag_8GeSe_6 and 21 mol% Ag_8SiSe_6, respectively):

$$L \Leftrightarrow \alpha' + \delta \; (T = 1120 - 1103K) \qquad (1)$$

3.4. Some polythermal sections of the phase diagram

Isopleth sections Ag_8SiSe_6–[A] (Fig. 7) and $5Ag_2Se$–[B] (Fig. 8) (where [A] is two-phase alloy in the Ag_2Se–$0.2Ag_8GeSe_6$ section with 50 mol% Ag_2Se; [B] is $Ag_8Si_{0.5}Ge_{0.5}Se_6$ solid solution) were studied in order to determine the crystallization sequence of the phases and the exact position of the monovariant line e_1e_2 and liquidus surface of the system.

The Ag_8SiSe_6-[A] section. The liquidus of this section consists of two curves (Figure 7). These curves correspond to the primary crystallization of the α' and δ solid solutions. At the point of intersection of those curves (5 mol% Ag_8SiSe_6), the α'+δ eutectic mixture crystallizes from the liquid. The monovariant process (1) occurs in a very small temperature range and has a sharp peak in the DTA curves. Therefore, the L+α'+δ three-phase area formed during the reaction (1) is delimited by a broken line. The reaction (1) ends with the formation of the two-phase field α'+δ. The horizontal line at 403K below the solidus corresponds to the polymorphic transformation of α' solid solutions based on the high-temperature modification of the Ag_2Se. The temperature of this transformation is constant and is the same with the corresponding transition temperature for the pure Ag_2Se. Near this transition temperature, both modifications of Ag_2Se indicate negligible solubility. A decrease in polymorphic transformation temperatures of Ag_8SiSe_6 and Ag_8GeSe_6 compounds is observed.

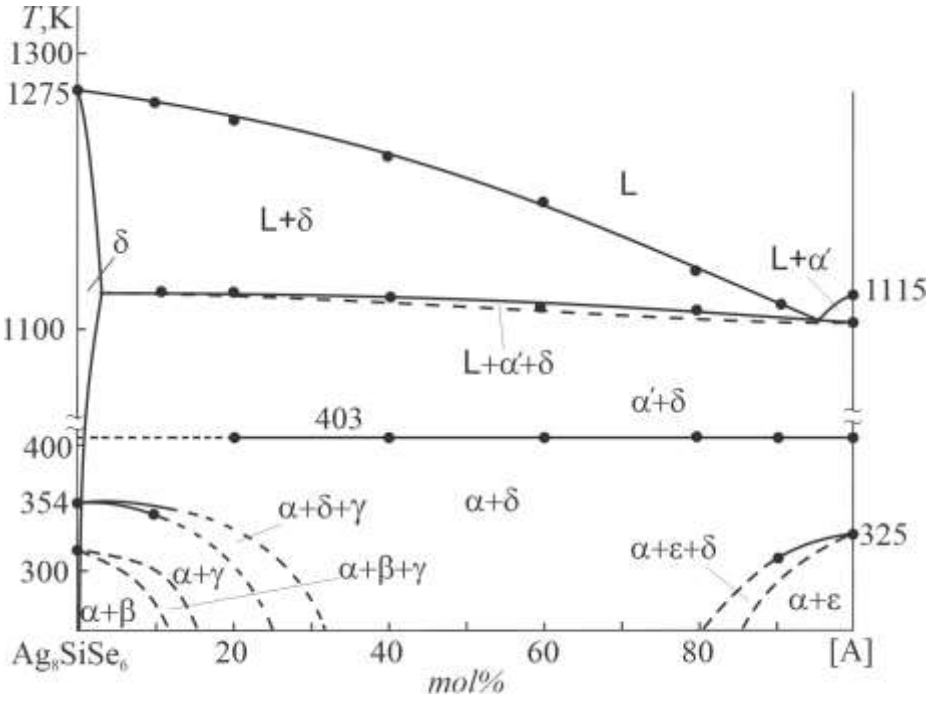

Fig.7. Isopleth section Ag_8SiSe_6-[A] ([A] is two-phase alloy in the $Ag_2Se–0.2Ag_8GeSe_6$ section with copmostion 50 mol% Ag_2Se)

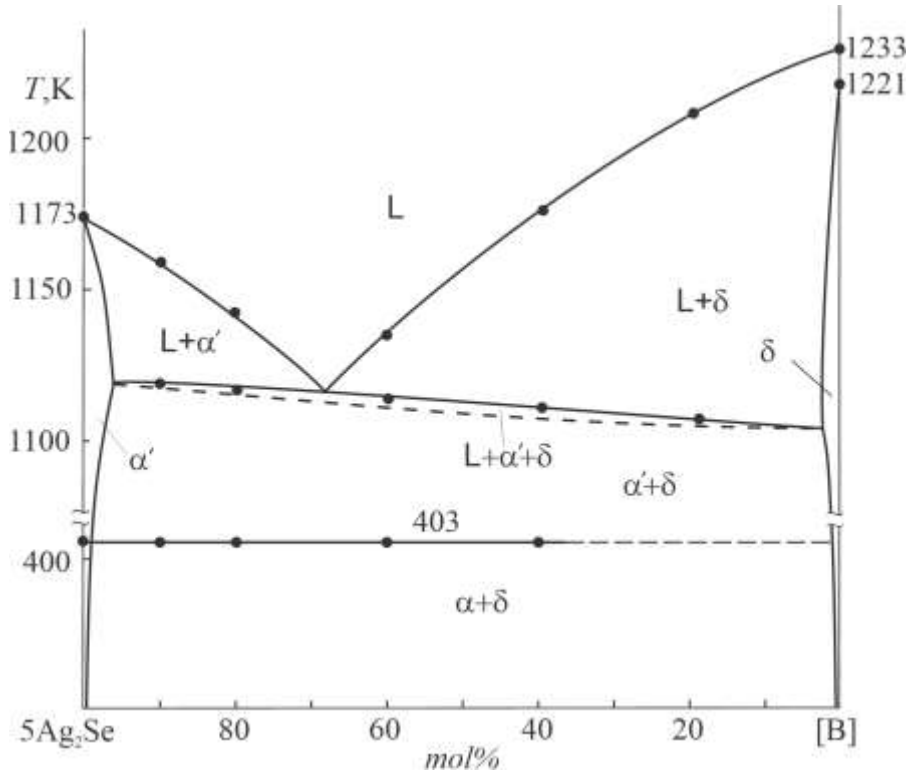

Fig. 8. Isolepth section Ag_2Se-[B] ([B] is $Ag_8Si_{0.5}Ge_{0.5}Se_6$ solid solution)

The Ag_2Se-[B] section. The picture of phase equilibria in this section is similar to the previous polythermal section (Fig. 8). This section also passes through the primary crystallization areas of α' and δ solid solutions. A monovariant eutectic equilibrium (1) is observed in the system below the liquidus, and a two-phase field α'+δ is formed. The horizontal line at 403K corresponds to the polymorphic transformation of Ag_2Se.

Conclusion

Here, a new picture of phase equilibria in the $Ag_2Se–Ag_8SiSe_6–Ag_8GeSe_6$ system was obtained. The diagram of the solid phase equilibria of the system at 300 K, the projection of the liquidus surface, as well as the T-x diagrams of the $Ag_8SiSe_6–Ag_8GeSe_6$ boundary system and two internal polythermal sections were constructed. In the $Ag_8SiSe_6–Ag_8GeSe_6$ system, continuous solid solutions (δ-phase) were found between the high-temperature modifications of the primary compounds with a cubic structure. It was determined that the formation of solid solutions is accompanied by a decrease in the polymorph transition temperatures of both compounds. This extends the lower limit of the homogeneity region of the ion-conducting δ-phase below room temperature. The fact that the liquidus surface of the δ-phase is very wide creates a good opportunity for growing single crystals of this phase by the directional crystallization method. It is also shown that the liquidus surface of the $Ag_2Se–Ag_8SiSe_6–Ag_8GeSe_6$ system consists of two areas corresponding to the initial crystallization of the (HT-Ag_2Se) and δ-phase.

References

1. Woodrow P. Chalcogenides: Advances in Research and Applications. Nova Science Publishers. 2018. 111 p.
2. Sanghoon X.L., Tengfei L.J., Zhang L.Y., Furdyna K. J. Chalcogenides: From 3D to 2D and beyond. Elsevier. 2019. 398 p.
3. Ahluwalia G.K. Applications of Chalcogenides: S, Se, and Te. Springer. 2016. 461 p.
4. Schwarzmüller S., Souchay D., Günther D., Gocke A., Dovgaliuk I., Miller S. A., Oeckler O. Argyrodite-Type Cu_8GeSe_6-xTex($0 \leq x \leq 2$): Temperature-Dependent Crystal Structure and Thermoelectric Properties. *Zeitschrift Für Anorganische Und Allgemeine Chemie*. 2018, vol. 644, no. 24, pp. 1915-1922. doi:10.1002/zaac.201800453
5. Acharya S., Soni A., High thermoelectric power factor in p-type Cu_8GeSe_6. *Solid state physics symposium.* 2019, vol. 2115, no. 1, pp. 1-3. doi.org/10.1063/1.5113463
6. Li W., Lin S., Ge B. Low Sound Velocity Contributing to the High Thermoelectric Performance of Ag_8SnSe_6. *Advanced Science.* 2016, vol. 3, no. 11, pp. 1600196-1600201. doi:10.1002/advs.201600196
7. Ghrib T., Otaibi A.L., Almessiere A., Assaker I. B. High Thermoelectric Figure of Merit of Ag_8SnS_6 Component Prepared by Electrodeposition Technique. *Chinese Physics Letters.* 2015, vol. 32, no 12, pp. 127402-127409. doi:10.1088/0256-307X/32/12/127402
8. Jin M., Lin S., Li W., Chen Z., Li R., Wang X., Pei Y. Fabrication and Thermoelectric Properties of Single-Crystal Argyrodite Ag_8SnSe_6. *Chemistry of Materials*. 2019, vol. 31, no. 7, pp. 2603–2610. doi:10.1021/acs.chemmater.9b00393
9. Shen X., Yang C., Liu Y., Wang G., Tan H., Tung Y.H., Zhou X. High-Temperature Structural and Thermoelectric Study of Argyrodite Ag_8GeSe_6. *ACS Applied Materials and Interfaces*. 2019, vol. 11, no. 2, pp. 2168–2176. doi:10.1021/acsami.8b19819
10. Charoenphakdee A., Kurosaki K., Muta H., Masayoshi U., Shinsuke Y. Ag_8SiTe_6: A New Thermoelectric Material with Low Thermal Conductivity. *Japanese Journal of Applied Physics.* 2009, vol. 48, no. 1, pp. 01160-01169. doi:10.1143/jjap.48.011603
11. Qinghui J., Suwei L., Yubo L., Wang L., Jonyou Y. Eco-friendly Highly Robust Ag_8SiSe_6-Based Thermoelectric

Composites with Excellent Performance Near Room Temperature. *ACS publications.* 2020, vol.12, no. 49, pp. 54653-54661. doi.org/10.1021/acsami.0c15877

12. Masaki F., Ken K., Hiroaki M., Shinsuke Y. Thermoelectric properties of Ag_8GeTe_6. *Journal of Alloys and Compounds.* 2005, vol. 396, no. 1, pp. 280–282. doi.org/10.1016/j.jallcom.2004.12.038
13. Semkiv I., Ilchuk H., Pawlowski M. Viktor K., Ag_8SnSe_6 argyrodite synthesis and optical properties. *Opto-Electronics Review*. 2017, vol. 25, no. 1, pp. 37–40. doi.org/10.1016/j.opelre.2017.04.002
14. Lu C., Zhang L., Zhang Y., Yang M., Shen-Ye L. Electronic, optical properties, surface energies and work functions of Ag_8SnS_6: First-principles method. *Chinese Physics B*. 2015, vol. 24, no. 1, pp. 1-7. Doi.10.1088/1674-1056/24/1/017501
15. Boon-on P., Aragaw B., Lee A., Chun-lin L., Shi B. Ag_8SnS_6: a new IR solar absorber material with a near -optimal bandgap. *RSC Advances.* 2018, vol. 8, no. 69, pp. 39470–39476. doi:10.1039/c8ra08734b
16. Brammertz G., Vermang B., ElAnzeery H., Sahayaraj S., Ranjbar S., Meuris M., Poortmans J. Fabrication and characterization of ternary Cu_8SiS_6 and Cu_8SiSe_6 thin film layers for optoelectronic applications. *Thin Solid Films*. 2016, vol. 616, no. 1, pp. 649–654. https://doi.org/10.1016/j.tsf.2016.09.049
17. Somnath A., Juhi P., Ajay S., Enhancement of Power Factor for Inherently Poor Thermal Conductor Ag_8GeSe_6 by Replacing Ge with Sn. *ACS Appl. Energy Mater*. 2019, vol. 2, no. 1, pp. 654–660. https://doi.org/10.1021/acsaem.8b01660
18. Tim B., Riley H., Bjoern W., Kazuki I., Siqi L., Michael G., Marius G., Martin P., Samuel G., Geoffroy H., Yanzhong P., Michael R., Gerhard W., G. Jeffrey S., Janine G., Matthias A., Wolfgang Z. Considering the Role of Ion Transport in Diffuson-Dominated Thermal Conductivity. *Advanced Energy Materials.* 2022, vol. 12, no. 22. pp. 2200717. https://doi.org/10.1002/aenm.202200717
19. Hull S., Berastegui P., Grippa A. Ag^+ diffusion within the rock-salt structured superionic conductor $Ag_4Sn_3S_8$. *Journal of Physics: Condensed Matter*. 2005, vol. 17, no 7. pp. 1067–1084. doi:10.1088/0953-8984/17/7/002
20. Heep B., Weldert S., Krysiak Y., Day W., Zeier G., Kolb U., Tremel W. High Electron Mobility and Disorder Induced by Silver Ion Migration Lead to Good Thermoelectric Performance in the Argyrodite Ag_8SiSe_6. *Chemistry of materials.* 2017, vol. 29, no. 11, pp. 4833−4839. doi:10.1021/acs.chemmater.7b00767
21. Boucher F., Evain M., Brec R. Distribution and Ionic Diffusion Path of Silver in γ-Ag_8GeTe_6: A Temperature Dependent Anharmonic Single Crystal Structure Study. *Journal of Solid State Chemistry*. 1993, vol. 107, no. 2, pp. 332–346. https://doi.org/10.1006/jssc.1993.1356
22. Sardarly R., Ashirov G. , Mashadiyeva L., Aliyeva N., Salmanov F., Agayeva R., Babanly M., Ionic conductivity of the Ag_8GeSe_6 compound. *Modern Physics Letters B.* 2023, vol. 36, no. 32, pp. 2250171. https://doi.org/10.1142/S0217984922501718
23. West D. R. F. Ternary Phase Diagrams in Materials Science. 3rd edition. CRC Press. 2019, 236 p.
24. Hiroyasu S. Introduction To Phase Diagrams In Materials Science And Engineering. World Scientific Publishing Company. 2020, 188 p.
25. Babanly M., Mashadiyeva L., Babanly D., Imamaliyeva S., Taghiyev D., Yusibov Y. Some issues of complex investigation of the phase equilibria and thermodynamic properties of the ternary chalcogenide systems by the EMF method. *Russian J.Inorg. Chem.* 2019, vol. 64. no. 13, pp.1649-1671. doi:10.1134/S0036023619130035
26. Imamaliyeva S., Babanly D., Tagiev D., Babanly M. Physicochemical Aspects of Development of Multicomponent Chalcogenide Phases Having the Tl_5Te_3 Structure: A Review. *Russ.J.Inorg.Chem.,* 2018, vol. 63, no. 13, pp.1703-1730.

27. Mansimova S.H., Babanly K.N., Mashadiyeva L.F., Mirzoyeva R.J., Babanly M.B. Phase equilibria in the Ag_2Se-PbSe-$AgSbSe_2$ system. *Chemical problems.* 2019, vol. 19, no. 1, pp. 41-49. doi.org/10.32737/2221-8688-2019-1-41-49
28. Alverdiyev I.J. Refinement of phase diagram in the Cu_2S-GeS_2 system. *Chemical problems*. 2019, vol. 17, no. 3, pp. 423-428. doi: 10.32737/2221-8688-2019-3-423-428
29. Mansimova S.H., Babanly K.N., Mashadiyeva L.F. Phase equilibria in the PbSe-$AgSbSe_2$ system. *Chemical problems*. 2018, vol. 16, no. 4, pp.530-536 . https://doi.org/10.32737/2221-8688-20 18-4-530-536
30. Mashadieva L., Alieva Z., Mirzoeva R. Yusibov Y., Shevel'kov A., Babanly M. Phase Equilibria in the $Cu_2Se–GeSe_2–SnSe_2$ System. *Russ. J. Inorg. Chem*. 2022, no. 67, pp. 670–682. https://doi.org/10.1134/S003602362205012 6
31. Alverdiyev I.J., Aliev Z.S., Bagheri S.M., Mashadiyeva L.F., Yusibov Y.A., Babanly M.B. Study of the $2Cu_2S+GeSe_2↔Cu_2Se+GeS_2$ reciprocal system and thermodynamic properties of the $Cu_8GeS_{6-x}Se_x$ solid solutions. *J.Alloys Compd.*, 2017, vol. 691, pp. 255-262. https://doi.org/10.1016/j.jallcom.2016.08.2 51
32. Alverdiev I.J., Bagheri S.M., Aliyeva Z.M., Yusibov Y.A., Babanly M.B. Phase equilibria in the $Ag_2Se–GeSe_2–SnSe_2$ system and thermodynamic properties of $Ag_8Ge_{1-x}Sn_xSe_6$ solid solutions. *Inorganic Materials*. 2017, vol. 53, no. 8, pp. 801–809. DOI:10.1134/S0020168517080027
33. Aliyeva Z.M., Bagheri S.M., Aliev Z.S., Yusibov Y.A., Babanly M.B. The phase equilibria in the $Ag_2S–Ag_8GeS_6–Ag_8SnS_6$ system. Z.M.Aliyeva. *Journal of Alloys and Compounds.* 2014, vol. 611, pp. 395–400. doi:10.1016/j.jallcom.2014.05.112
34. Bagheri S.M., Imamaliyeva S.Z., Mashadiyeva L.F., Babanly M.B. Phase equilibria in the Ag_8SnS_6-Ag_8SnSe_6 system. *International Journal of Advanced Scientific and Technical Research* (India). 2014, vol 2, no. 4, pp. 291-296
35. Bayramova U.R., Poladova A.N., Mashadiyeva L.F. Synthesis And X-RAY study of the $Cu_8Ge_{(1-X)}Si_XS_6$ solid solutions. *New Materials, Compounds & Applications*. 2022, vol. 6, no. 3, pp. 276-281.
36. Alieva Z.M., Bagkheri S.M., Alverdiev I.J., Yusibov Y.A., Babanly M.B. Phase equilibria in the pseudoternary system Ag_2Se-Ag_8GeSe_6-Ag_8SnSe_6. *Inorganic Materials*, 2014, vol. 50, no. 10, pp. 1063–1068. DOI:10.1134/S002016851410001X
37. Ashirov G.M. Phase equilibria in the $Ag_8SiTe_6–Ag_8GeTe_6$ system. *Azerbaijan Chemical Journal.* 2022, no. 1, pp. 89-93. doi.org/10.32737/0005-2531-2022-1-89-93
38. Karakaya I., Thompson W. T. The Ag-Se (Silver-Selenium) system. *Bulletin of Alloy Phase Diagrams*. 1990. no.11, pp. 266–271. https://doi.org/10.1007/BF03029297
39. Hofmann A. Silver-Selenium-Silicon. *Ternary Alloys*. 1988, pp. 559-560.
40. Gorochov O. Les composés $A_{g8}MX_6$ (M= Si, Ge, Sn et X= S, Se, Te). *Bulletin de la Société Chimique de France.* 1968, no. 101, pp.2263-2275.
41. Venkatraman M., Blachnik R., Schlieper A. The phase diagrams of M_2X -SiX_2 (M is Cu, Ag; X is S, Se). *Thermochimica Acta*. 1995, no. 249, pp. 13-20. https://doi.org/10.1016/0040-6031(95)90666-5
42. Piskach L.V., Parasyuk O.V., Olekseyuk I.D., Romanyuk Y.E. Volkov S.V., Pekhnyo V.I. Interaction of argyrodite family compounds with the chalcogenides of II-b elements. *Journal of Alloys and Compounds*. 2006, vol. 421, no. 1, pp. 98-104. https://doi.org/10.1016/j.jallcom.2005.11.0 56
43. Amiraslanova A.J., Babanly K.N., Imamaliyeva S.Z., Yusibov Y.A., Babanly M.B. Phase equilibria in the Ag_8SiSe_6- Ag_8SiTe_6 system and characterization of solid solutions $Ag_8SiSe_{6-x}Te_x$. *Applied Chemical Engineering*, 1023, vol. 6, no.2. DOI: http://dx.doi.org/10.24294/ace.v6i2.216 2
44. Carré D., Ollitrault F. R., Flahaut J.

Structure de Ag_8GeSe_6 β. *Acta Crystallogr., Sect. B: Struct.Crystallogr. Cryst. Chem.*, 1980, vol. 36, no. 2, pp. 245–249. https://doi.org/10.1107/S0567740880003032

45. Prince A., Silver–Germanium–Selenium: Ternary Alloys VCH, Weinheim, Germany, 1988, 195–210 p.
46. Yusibov Y. A., Alverdiev I.D., Ibragimova F.S., Mamedov A.N., Tagiev D.B., Babanly M.B. Study and 3D modeling of the phase diagram of the Ag–Ge–Se system. *Russian Journal of Inorganic Chemistry*. 2017, vol. 62, no. 9, pp. 1223–1233. https://doi.org/10.1134/S0036023617090182

ФАЗОВЫЕ РАВНОВЕСИЯ В СИСТЕМЕ $Ag_2Se–Ag_8GeSe_6–Ag_8SiSe_6$ И ХАРАКТЕРИСТИКА ТВЕРДЫХ РАСТВОРОВ $Ag_8Si_{1-x}Ge_xSe_6$

[1]Г.М. Аширов, [1]К.Н. Бабанлы, [1]Л.Ф. Машадиева, [2]Ю.А. Юсибов, [1]М.Б. Бабанлы

[1]Институт Катализа и Неорганической Химии им. акад. М.Нагиева
AZ 1143 Баку, пр.Г.Джавида, 113, Баку, Азербайджан
[2]Гянджинский Государстенный Университет
Пр. Г.Алиева, 429, Гянджа, Азербайджан
e-mail : leylafm76@gmail.com

Аннотация: Методами дифференциально-термического и рентгенофазового анализов изучены фазовые равновесия в системе $Ag_2Se–Ag_8SiSe_6–Ag_8GeSe_6$. На основании экспериментальных результатов и литературных данных построены проекция поверхности ликвидуса системы $Ag_2Se–Ag_8SiSe_6–Ag_8GeSe_6$, изотермический разрез при 300 К и некоторые политермические сечения фазовой диаграммы. Установлено, что на боковой системе $Ag_8SiSe_6–Ag_8GeSe_6$ концентрационного треугольника образуются непрерывный ряд твердых растворов на основе высокотемпературной кубической модификации исходных соединений, и ограниченные твердые растворы – на основе их низкотемпературных модификаций. Образование твердых растворов приводит к резкому снижению температур полиморфных переходов тройных соединений и стабилизации высокотемпературных фаз при комнатной температуре. Поверхность ликвидуса системы $Ag_2Se–Ag_8SiSe_6–Ag_8GeSe_6$ состоит из 2 областей, отражающих первичные кристаллизации α'-фазы на основе НТ-Ag_2Se и твердых растворов НТ-$Ag_8Si_{1-x}Ge_xSe_6$. Полученные новые фазы представляют интерес как экологически безопасные материалы с термоэлектрическими свойствами и смешанной ионно-электронной проводимостью.

Ключевые слова: соединения семейства аргиродита, селенид серебра-германия, селенид серебра-кремния, фазовые равновесия, поверхность ликвидуса, твердые растворы, Т-х диаграмма, параметры кристаллической решетки.

$Ag_2Se–Ag_8GeSe_6–Ag_8SiSe_6$ SİSTEMİNDƏ FAZA TARAZLIĞI VƏ $Ag_8Si_{1-x}Ge_xSe_6$ BƏRK MƏHLULLARIN XARAKTERİSTİKASI

[1] G.M. Əşhirov, [1] K.N. Babanlı, [1] L.F. Məşədiyeva, [2]Y.A. Yusibov, [1] M.B. Babanlı

[1]Akad. M.Nağıyev adına Kataliz və Qeyri-üzvi Kimya İnstitutu
AZ 1143, Bakı, H.Cavid pr., 113
[2]Gəncə Dövlət Universiteti
Gəncə ş., H .Əliyev pr., 429
e-mail : leylafm76@gmail.com

Xülasə: $Ag_2Se–Ag_8SiSe_6$ – Ag_8GeSe_6 sistemində faza tarazlıqları diferensial termiki analiz və rentgen faza analizi üsulları ilə tədqiq edilmişdir. Eksperimental nəticələr və ədəbiyyat məlumatları əsasında $Ag_2Se–Ag_8SiSe_6$ – Ag_8GeSe_6 sisteminin likvidus səthinin proyeksiyası, faza diaqramının 300 K-də izotermik kəsiyi və bəzi politermik kəsikləri qurulmuşdur. Müəyyən edilmişdir ki, qatılıq üçbucağının Ag_8SiSe_6 – Ag_8GeSe_6 yan tərəfində ilkin birləşmələrin yüksək temperaturlu kubik modifikasiyaları arasında fasiləsiz, aşağı temperaturlu modifikasiyaları əsasında isə məhdud bərk məhlul sahələri əmələ gəlir. Bərk məhlulların əmələ gəlməsi birləşmələrin polimorf keçid temperaturlarının kəskin azalması və yüksək temperaturlu fazaların otaq temperaturunda stabilləşməsinə gətirib çıxarır. $Ag_2Se–Ag_8SiSe_6$ – Ag_8GeSe_6 sisteminin likvidus səthi HT- Ag_2Se əsasında α'- fazanın və HT-$Ag_8Si_{1-x}Ge_xSe_6$ bərk məhlullarının ilkin kristallaşmasını əks etdirən 2 sahədən ibarətdir. Alınmış yeni fazalar termoelektrik xassələrə və qarışıq ion-elektron keçiriciliyinə malik ekoloji təhlükəsiz materiallar kimi maraq kəsb edir.

Açar sözlər: arqirodit ailəsi birləşmələri, gümüş-germanium selenidi, gümüş-silisium selenidi, faza tarazlıqları, likvidus səthi, bərk məhlullar, T-x diaqramı, kristal qəfəs parametrləri.